Bioorganic & Medicinal Chemistry Letters 25 (2015) 2335–2339

Contents lists available at ScienceDirect

Bioorganic & Medicinal Chemistry Letters

journal homepage: www.elsevier.com/locate/bmcl

Identification of lead compounds for ^{99m}Tc and ^{18}F GPR91 radiotracers

Jeffrey Klenc *, Malgorzata Lipowska, Andrew T. Taylor

Department of Radiology and Imaging Sciences, Emory University, Atlanta, GA 30322, USA

ARTICLE INFO

Article history:
Received 26 January 2015
Revised 1 April 2015
Accepted 8 April 2015
Available online 11 April 2015

Keywords:
GPR91
Radiotracer
Hyperglycemia
Hypoxia
Diabetes
Lead identification

ABSTRACT

To develop the first radiotracer targeting GPR91, a cell membrane-bound receptor that modulates the cellular response to hyperglycemia and hypoxia, we designed and prepared a small series of compounds based on a published series of 1,8-naphthyridines with high affinity to GPR91. Our approach provides a mechanism to incorporate radioactive atoms (^{99m}Tc and ^{18}F) into the GPR91 pharmacophore as the final synthetic step. Pharmacological assays confirmed lead compounds for ^{99m}Tc and ^{18}F GPR91 radiotracers within the series.

The membrane-bound receptor GPR91 has a major role in the cellular response to hyperglycemia and hypoxia due to its ability to bind the citric acid cycle intermediate, succinate.[1,2] As glycolysis increases, succinate is transported from the site of glycolysis in the mitochondria to the intracellular environment; from the intracellular environment, succinate is transported across the cell membrane to the extracellular space, where it effects a paracrine-like response through activation of GPR91.[1] The activation of GPR91 then initiates a variety of common cell-signaling pathways (p38, ERK 1/2, COX-2, etc.) stimulating cells that express the receptor to alter their local environments.

GPR91 activation by succinate has therefore been linked to various cell stress responses.[3,4] For example, activation of GPR91 expressed on macula densa cells in the kidney leads to the release of prostaglandin E_2; prostaglandin E_2 via paracrine signaling causes increased renin synthesis and release from the adjacent juxtaglomerular cells with subsequent activation of the renin–angiotensin system (RAS).[1,5] RAS activation may contribute to renal damage and has been correlated to the onset and progression of diabetic nephropathy.[6] Similarly, activation of GPR91 expressed on retinal ganglion cells leads to the production of vascular endothelial growth hormone and the consequent release of angiotensin I/II, causing angiogenesis in retinal tissues which may contribute to the progression of diabetic retinopathy,[7] a leading cause of blindness in American adults.

GPR91 is also widely expressed throughout vascularized tissues, and many of the receptor's roles in these tissues have not been characterized.[8,9] Although researchers continue to work toward characterizing the role of GPR91, studies remain limited to in vitro and ex vivo methods, or in vivo fluorescence microscopy of secondary markers of GPR91 activation.[5,10] Currently, there is no GPR91 imaging agent for directly characterizing receptor expression in vivo. Such an agent would allow researchers to monitor changes in GPR91 expression in relevant models to enhance our understanding of pathophysiology and facilitate drug development efforts.[11]

We have undertaken the development of a GPR91 radiotracer by preparing a small series of compounds based on the published series of 1,8-naphthyridine compounds with high affinity to GPR91.[12] Although many radionuclides offer unique advantages for receptor imaging, ^{99m}Tc and ^{18}F each have especially attractive properties,[13,14] including their widespread availability, practical half-life (6 h and 110 min, respectively), variety of radiosynthetic approaches,[15,16] and high image quality for small animal imaging studies. Additionally, ^{99m}Tc and ^{18}F have close nonradioactive structural analogs (Re and ^{19}F, respectively) that alleviate some of the practical difficulty of working with radioactive compounds during preliminary structural and pharmacological characterizations.

Abbreviations: GPR91, G-protein coupled receptor; HPLC, high-performance liquid chromatography; HRMS, high resolution mass spectrometry.

* Corresponding author. Tel.: +1 678 360 0352.
E-mail address: jeff.klenc@gmail.com (J. Klenc).

http://dx.doi.org/10.1016/j.bmcl.2015.04.015
0960-894X/

Therefore, we sought to identify suitable lead compounds within a series of Re and ^{19}F compounds described herein as a step toward the further exploration of GPR91 expression in hypoxic and hyperglycemic models.

The design of this series of nonradioactive analogs of potential GPR91 radiotracers (Fig. 1) relied on structure–activity relationship data from a recently published series of 1,8-naphthyridine compounds with high affinity for the GPR91 receptor.[12] The literature demonstrated that the biphenyl region was most tolerant to modification, while any perturbation to the distant 1,8-naphthyridinyl region resulted in a significant loss in affinity. Therefore, we aimed to replace the biphenyl moiety of the 1,8-naphthyridines with a Re chelate sphere or a structurally similar biphenyl group amenable to common ^{18}F labeling reactions (Fig. 1). The linker length for metal complexes was also varied ($n = 3$ or 4) in an effort to ensure the spacing between the 1,8-naphthyridine and the modified biphenyl region remained consistent with the published series of GPR91 ligands.

Further, we chose to incorporate M (M = ^{99m}Tc/Re) into the proposed derivatives as an $M^{I}(CO)_3$ core in order to yield smaller metal complexes which may fit more easily within the GPR91 binding site. Previous examples of $M^{I}(CO)_3$ complexes that bind to a structurally related G-protein coupled receptor with high affinity (nM) support this approach.[17] Additionally, the $[M(CO)_3(H_2O)_3]^+$ precursor is able to bind a tridentate ligand in a predictable manner and yield the desired tridentate $M^{I}(CO)_3$ complexes by a method that is also practical for ^{99m}Tc radiolabeling.[18] As shown in Scheme 1, this strategy led to the preparation of four $Re^{I}(CO)_3$ complexes (**9a–b** and **10a–b**) having a neutral or negative overall charge and a linker length of 3 or 4 carbons. Reaction of tridentate ligands **8a–b** with the $[Re(CO)_3(H_2O)_3]^+$ precursor yielded **10a–b** as the major products under conditions analogous to ^{99m}Tc radiolabeling. The synthesis of **9a–b** via amide coupling of **5a–b** with the Re complex **7** offers an alternative route to nonradioactive analogs to expedite lead optimization.

For the preparation of reference compound **14**, we deviated from the previously reported route[12] by using a Suzuki coupling between **13** and commercially available 3-iodotoluene in the final step (Scheme 2). This route avoids substitution of the nitro leaving group prior to the intended nucleophilic substitution with TBAF, and also provides an efficient approach to diversify the aryl ring of the biphenyl moiety in future generations of potential GPR91 ligands. The boronic acid **13** was reacted with commercially available 4-iodo-2-nitropyridine to yield **15** in a single step as a precursor for a fluorination reaction. When **15** was heated with TBA^{19}F, the starting material was largely consumed after 15 min and the fluorinated product **16** was then isolated from the reaction mixture in high purity by HPLC, validating our planned radiosynthetic approach and providing **16** as a model for preparation of an ^{18}F tracer.

The nonradioactive test compounds **9a–b**, **10a–b**, and **16** were then evaluated in vitro as potential agonists and antagonists of GPR91 using a calcium-flux luminescent assay (as described in detail in Supplementary data). Briefly, an increase in the fluorescence of the cell-containing mixture as the test compound was added would indicate an agonist response, whereas the absence of a response would indicate no agonism. None of the test compounds exhibited agonism of GPR91 as expected from the results of the previously reported series of 1,8-naphtyridines on which these compounds were designed.[12] Antagonism was characterized by the ability of the test compound to inhibit the increase in fluorescence due to addition of the natural GPR91 agonist (succinate, 100 μM). Serial aqueous dilutions of the test compounds were prepared in order to assay the compounds for GPR91 antagonism. Negatively charged compounds dissolved easily, whereas neutral compounds **10a–b** and **16** began to precipitate out of the 5% DMSO aqueous solution at concentrations above ~100 μM. Reference compound (**14**) showed a strong inhibition of the agonist response of succinate as expected (IC_{50} = 265 nM), comparable to that previously reported.[12] Incubation with serial dilutions of novel compounds **10a–b** and **16** produced a moderate inhibition (IC_{50} = 25 μM, 18 μM, and 21 μM, respectively) as shown in Figure 2; whereas compounds **9a–b** had no effect on the agonist response at any concentration (IC_{50} > 100 μM). The Hill coefficients for compounds **10a–b** and **14** were near 1 as expected for antagonists which bind competitively at the GPR91 binding site. However, fitting the data from compound **16** gave a steep Hill slope, possibly indicating that the ligand has a more complicated mechanism of GPR91 inhibition. However, in view of the results from compounds **10a–b**, **14** and those previously published,[12] we find it more likely that the steep slope observed for **16** is the result of a lack of data points at higher concentrations, which were unable to be obtained due to solubility issues.

Comparisons between the in vitro activity of **10a** and **10b** suggest that the effect of the linker length was minimal, although compound **10b** ($n = 4$) showed slightly higher antagonism than compound **10a** ($n = 3$). The results also suggest that the negative charge of compounds **9a–b** led to an unfavorable binding interaction at the GPR91 binding site, as the size of Re complexes **9** and **10** are comparable. Future generations of GPR91 ligands may therefore benefit from the inclusion of polar groups in the linker region to aid solubility while avoiding a negative charge in the biphenyl region of the ligand. Compounds which contain a positive charge may also offer an alternative to increasing solubility without suffering losses in affinity as demonstrated by the negatively charged compounds of this series.

Finally, as a proof of concept, we conducted the radiolabeling of **8a** and biodistribution studies with the resulting ^{99m}Tc tracer, according to protocols comparable to those in our concurrent research to develop renal imaging agents.[19,20] Radiolabeling of **8a**

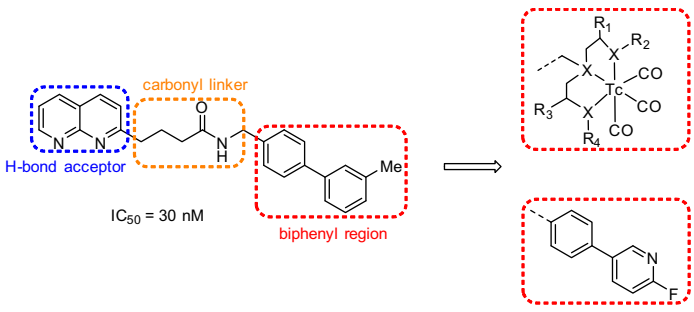

Figure 1. General pharmacophore for GPR91 antagonists with high affinity.[12] Bhuniya et al. showed that modifications to the biphenyl region and carbonyl linker were well-tolerated compared to changes in the hydrogen bond accepting 1,8-naphthyridine moiety.

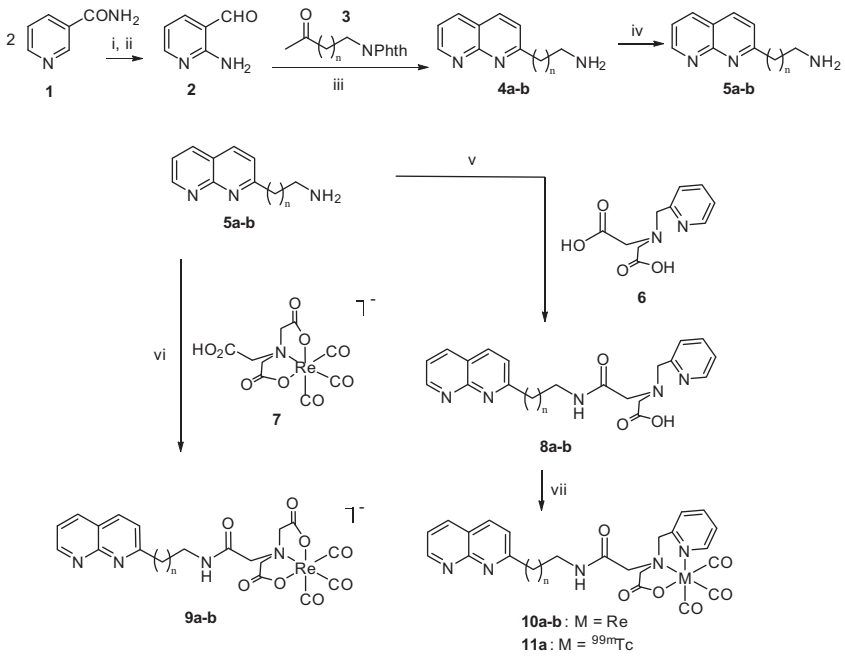

Scheme 1. Synthesis of complexes **9**–**11**. Reagents and conditions: (i) ammonium sulfamate, 200 °C, 5 h; (ii) 2 N HCl; (iii) L-proline, abs EtOH, 70 °C, 18 h; (iv) $MeNH_2$, EtOH, 70 °C, 5 h; (v) *N*-[(pyridin-2-yl)methyl]iminodiacetic acid, BOP-Cl, THF, TEA; (vi) BOP, TEA, DMF, 3 d, followed by a mild deprotection; (vii) $[M(CO)_3(H_2O)_3]OTf$, 70 °C, 30 min, pH 7. (a) $n = 3$, (b) $n = 4$.

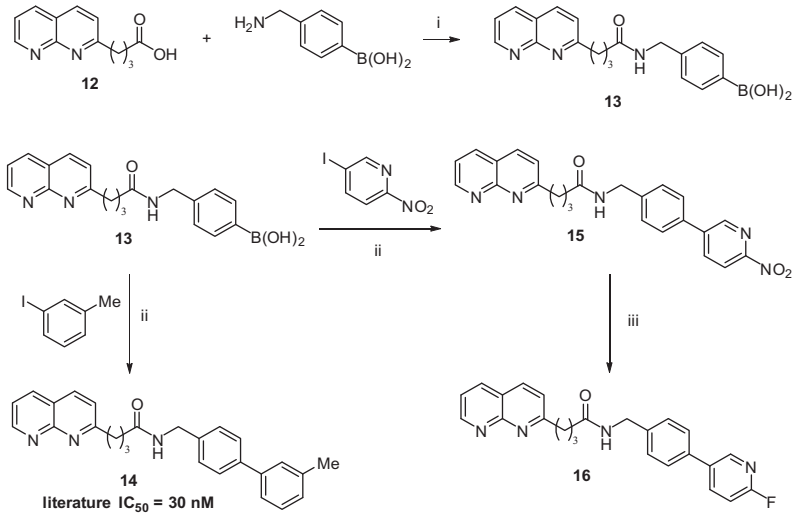

Scheme 2. Synthesis of the ^{19}F lead compound **16** and an alternate synthesis of **14** than previously reported[12] as a reference compound for the GPR91 inhibition assay. Reagents and conditions: (i) BOP, DIPEA, DMF, rt, 24 h; (ii) $Pd(OAc)_2$, PPh_3, $NaHCO_3$, $MeOH/H_2O$, reflux, 4 h; (iii) TBAF, 70 °C, 15 min.

(Scheme 1) produced the tracer **11a** as a single product with high radiochemical purity (>99%). The identity of **11a** was confirmed by coinjecting it on HPLC with the non-radioactive Re analog **10a**; the Re and ^{99m}Tc complexes had similar retention times (19.2 and 19.6 min, respectively). The stability of **11a** was examined in a physiological phosphate buffer at pH 7.4 by analyzing of an aliquot of the incubating sample over the time. HPLC analysis revealed only **11a** after 24 h indicating the product was stable under physiological conditions (Fig. 3). Biodistribution studies with **11a** at 10, 60, and 120 min post-injection revealed that most of **11a** was eliminated via the hepatobiliary pathway, but a significant portion of the dose was excreted via the kidney (20–25%, Table 1), indicating that **11a** reached GPR91 expressed on macula densa cells in the kidney. However, only a marginal increase in radioactivity in the kidney compared to the background was observed at each time point, suggesting that the affinity of **11a** to GPR91 must be improved to afford a viable GPR91 tracer.

The presented data identified compounds **10a**–**b** and **16** as lead compounds for ^{99m}Tc and ^{18}F tracers with moderate affinity to GPR91. In addition, we validated our synthetic approach through the successful ^{99m}Tc radiolabeling of **8a** and the inclusion of ^{19}F into **16** as a model for preparation of an ^{18}F tracer. Biodistribution studies with **11a** demonstrated that the tracer was excreted by the kidney, suggesting that the tracer reached the GPR91-expressing macula densa cells. Compound **11a** therefore represents an important step in the development of a novel

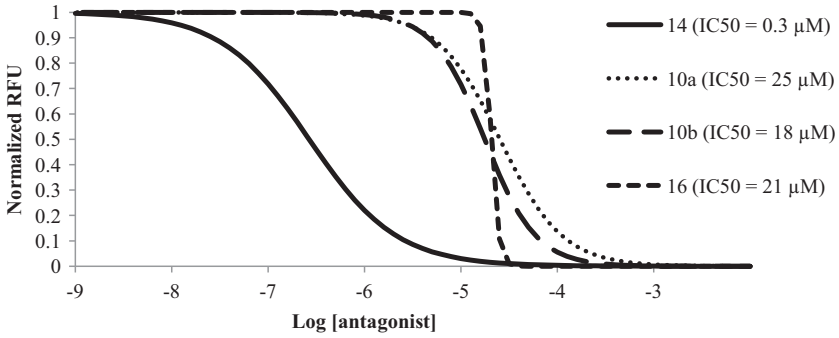

Figure 2. Dose–response curves for **10a–b**, **14** and **16** as calculated from the in vitro cell inhibition assay, represented as the relative fluorescence versus antagonist concentration. Data from reference compound **14** was comparable to previously published results.[12] Compounds **10a–b** and **16** showed a moderate antagonism (IC_{50} = 25 μM, 18 μM, and 21 μM, respectively). Dose–response curves for **9a–b** were unable to be calculated due to a lack of antagonism at all examined concentrations.

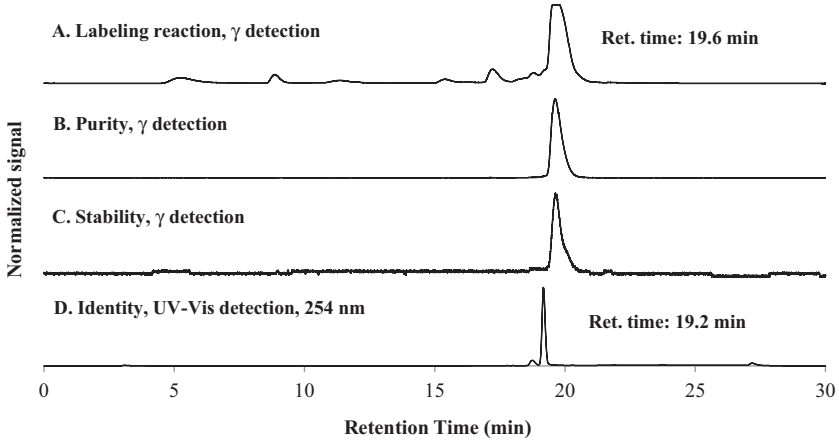

Figure 3. HPLC chromatograms after normalization from raw radioactivity units (A–C; γ detection) or absorption units (D; UV–Vis detection, 253 nm) detailing the preparation of **11a** via a $^{99m}Tc(CO)_3$ radiolabeling reaction. (A) The chromatogram from the **11a** labeling mixture after heating for 15 min shows the product as the major peak at 19.6 min. (B) The collected fraction has no significant peaks aside from **11a**. (C) After being stored at physiological conditions for 24 h, **11a** remains intact and shows no degradation. (D) The identity of **11a** is confirmed by co-injection with the fully characterized non-radioactive rhenium analog, **10a**. The retention time of the Re analog **10a** (19.2 min) appears slightly before the radioactive product **11a** because the UV detector is installed ahead of the radioactivity detector in the flow line.

Table 1
Percent injected dose of 11a in blood, urine and selected organs at 10, 60 and 120 min after injection in normal rats

	Blood	Kidney	Urine	Liver	Bowel[§]
10 min	1.4 ± 0.3	2.3 ± 0.8	15.8 ± 5.2	6.4 ± 0.4	49.3 ± 2.5
60 min	0.2 ± 0.0	0.6 ± 0.0	24.6 ± 3.1	3.4 ± 0.6	52.3 ± 2.1
120 min	0.2 ± 0.1	0.2 ± 0.0	22.5 ± 1.8	3.1 ± 0.1	35.7 ± 18.7

Data are presented as mean ± SD. 10 min and 120 min, n = 2, 60 min, n = 3.
[§] Bowel includes intestines and stomach.

research tool for investigating the GPR91 receptor in vivo and further optimization is warranted to identify ^{99m}Tc and ^{18}F GPR91 radiotracers with acceptable affinity to the receptor for in vivo imaging.

Acknowledgments

This research was funded by the Education and Research Foundation for Nuclear Medicine and Molecular Imaging, Inc. through the 2012 Mitzi and William Blahd, MD Pilot Research Grant. Additional support was received from the National Institute of Health/National Institute of Diabetes and Digestive and Kidney Diseases (Grant No. R37 DK38842). The authors also gratefully acknowledge Eugene Malveaux's surgical expertise in conducting the biodistribution studies. Additionally, we thank Dr. Randy Hall, Dr. Ray Dingledine and Dr. Asheebo Rojas for their guidance and access to equipment that enabled us to conduct the pharmacological assays.

Supplementary data

Supplementary data (complete details of the preparation and characterization of compounds, in vitro affinity assays, radiolabeling and biodistribution of **11a**) associated with this article can be found, in the online version, at http://dx.doi.org/10.1016/j.bmcl.2015.04.015.

References and notes

1. Peti-Peterdi, J. *Kidney Int.* **2010**, *78*, 1214.
2. He, W.; Miao, F. J. P.; Lin, D. C. H.; Schwandner, R. T.; Wang, Z.; Gao, J.; Chen, J.-L.; Tian, H.; Ling, L. *Nature* **2004**, *429*, 188.
3. Ariza, A. C.; Deen, P. M. T.; Robben, J. H. *Front. Endocrinol.* **2012**, *3*, 22.
4. Sadagopan, N.; Li, W.; Roberds, S. L.; Major, T.; Preston, G. M.; Yu, Y.; Tones, M. A. *Am. J. Hypertens.* **2007**, *20*, 1209.
5. Vargas, S. L.; Toma, I.; Kang, J. J.; Meer, E. J.; Peti-Peterdi, J. *J. Am. Soc. Nephrol.* **2009**, *20*, 1002.
6. Van Buren, P. N.; Toto, R. *Adv. Chronic Kidney Dis.* **2011**, *18*, 28.
7. Sapieha, P.; Sirinyan, M.; Hamel, D.; Zaniolo, K.; Joyal, J.-S.; Cho, J.-H.; Honore, J.-C.; Kermorvant-Duchemin, E.; Varma, D. R.; Tremblay, S.; Leduc, M.; Rihakova, L.; Hardy, P.; Klein, W. H.; Mu, X.; Mamer, O.; Lachapelle, P.; Di Polo, A.; Beausejour, C.; Andelfinger, G.; Mitchell, G.; Sennlaub, F.; Chemtob, S. *Nat. Med.* **2008**, *14*, 1067.
8. Regard, J. B.; Sato, I. T.; Coughlin, S. R. *Cell* **2008**, *135*, 561.

9. Correa, P. R. A. V.; Kruglov, E. A.; Thompson, M.; Leite, M. F.; Dranoff, J. A.; Nathanson, M. H. *J. Hepatol.* **2007**, *47*, 262.
10. Prokai, A.; Peti-Peterdi, J. *Front. Biosci.* **2010**, *2*, 1227.
11. Eckelman, W. C. *Nucl. Med. Biol.* **2002**, *29*, 777.
12. Bhuniya, D.; Umrani, D.; Dave, B.; Salunke, D.; Kukreja, G.; Gundu, J.; Naykodi, M.; Shaikh, N. S.; Shitole, P.; Kurhade, S.; De, S.; Majumdar, S.; Reddy, S. B.; Tambe, S.; Shejul, Y.; Chugh, A.; Palle, V. P.; Mookhtiar, K. A.; Cully, D.; Vacca, J.; Chakravarty, P. K.; Nargund, R. P.; Wright, S. D.; Graziano, M. P.; Singh, S. B.; Roy, S.; Cai, T.-Q. *Bioorg. Med. Chem. Lett.* **2011**, *21*, 3596.
13. Shah, P.; Westwell, A. D. *J. Enzyme Inhib. Med. Chem.* **2007**, *22*, 527.
14. Arano, Y. *Ann. Nucl. Med.* **2002**, *16*, 79.
15. Klenc, J. *Mol. Imaging Gateway* **2014**, *8*, 1.
16. Ermert, J. *BioMed. Res. Int.* **2014**, *2014*, 15.
17. Chiotellis, A.; Tsoukalas, C.; Pelecanou, M.; Pirmettis, I.; Papadopoulos, M. *Radiochim. Acta* **2011**, 307.
18. He, H.; Lipowska, M.; Xu, X.; Taylor, A. T.; Carlone, M.; Marzilli, L. G. *Inorg. Chem.* **2005**, *44*, 5437.
19. Lipowska, M.; Marzilli, L. G.; Taylor, A. T. *J. Nucl. Med.* **2009**, *50*, 454.
20. Lipowska, M.; Klenc, J.; Marzilli, L. G.; Taylor, A. T. *J. Nucl. Med.* **2012**, *53*, 1277.